

Synthesis and reactivity of dinuclear iron–platinum, chromium–platinum, molybdenum–platinum and tungsten–platinum complexes with bridging carbonyl, isocyanide and aminocarbyne ligands. An empirical study on the parameters decisive for the bonding mode of the isocyanide ligand

Michael Knorr^{a,*}, Isabelle Jourdain^a, Dieter Lentz^b, Stefan Willemsen^b,
Carsten Strohmann^c

^a Laboratoire de Chimie des Matériaux et Interfaces, Université de Franche-Comté, Faculté des Sciences et des Techniques, 16, Route de Gray, 25030 Besançon Cedex, France

^b Institut für Anorganische und Analytische Chemie, Freie Universität Berlin, Fabeckstrasse 34-36, D-14195 Berlin, Germany

^c Institut für Anorganische Chemie der Universität Würzburg, Am Hubland, D-97074 Würzburg, Germany

Received 24 April 2003; received in revised form 2 July 2003; accepted 2 July 2003

Dedicated to Prof. E.O. Fischer on the occasion of his 85th birthday

Abstract

The dppm-bridged heterobimetallic μ -carbonyl complexes $[(OC)_4M(\mu-CO)(\mu-dppm)Pt(PPh_3)]$ (**1a**, M = Cr; **1b**, M = Mo; **1c**, M = W) have been prepared by the reaction of $[M(CO)_5(\eta^1-dppm)]$ (M = Cr, Mo, W) with $[Pt(CH_2CH_2)(PPh_3)_2]$. The outcome of stoichiometric isocyanide addition to **1** is electronically controlled by the π -accepting propensity of CNR. Addition of isocyanide ligands with strongly electron withdrawing substituents R affords the isonitrile-bridged complexes $[(OC)_4M(\mu-C=N-R)(\mu-dppm)Pt(PPh_3)]$ **2** (M = W; R = CF₃), **3** (**3a**, M = Cr; **3b**, M = Mo, **3c**, M = W; R = CH₂SO₂*p*-tolyl), and **4** (M = W; R = [CH₂PPh₃][PF₆]). With less π -accepting isocyanides (R = CH₂Ph, C₆H₁₁, CH₂PO(OEt)₂), the labile complexes $[(RNC)(OC)_3W(\mu-C=O)(\mu-dppm)Pt(PPh_3)]$ (**5–7**) ligated by a terminal isonitrile ligand are formed. In contrast, treatment of $[(OC)_3Fe(\mu-CO)(\mu-dppm)Pt(PPh_3)]$ with CNCH₂PO(OEt)₂ yields exclusively $[(OC)_3Fe\{\mu-C=NCH_2PO(OEt)_2\}(\mu-dppm)Pt(PPh_3)]$ (**9**) with the isocyanide ligand in a bridging bonding mode. Upon protonation of **2** and **3b** with HBF₄, the stable μ -aminocarbyne complexes $[(OC)_4M(\mu-C=N(H)R)(\mu-dppm)Pt(PPh_3)][BF_4]$ (**10–11**) are formed by electrophilic addition of H⁺ on the basic isonitrile nitrogen atom. The molecular structures of **1a,c**, **2** and **3c** have been determined by X-ray diffraction methods. The μ -CO and the μ -CNR ligands bridge the metal centres in an asymmetric manner, the Pt– μ -C distances being significantly shorter than the corresponding M– μ -C distances. In contrast, the μ -CNCH₂PO(OEt)₂ ligand of $[(OC)_3Fe\{\mu-C=N-CH_2PO(OEt)_2\}(\mu-dppm)Pt(PPh_3)]$ (**9**) bridges symmetrically the two metal centres. Furthermore, the molecular structure of *cis*-[(benzylNC)(OC)₄W(η^1 -dppm)] (**8a**) resulting from degradation of **5** has been determined.

© 2003 Elsevier B.V. All rights reserved.

Keywords: Isocyanide; Platinum; Tungsten; Molybdenum; Chromium; Iron; Metal–metal bonds

1. Introduction

A common strategy to control ligand arrangements, reactivity patterns and catalytic activity of mononuclear phosphane complexes consists in variation of the electronic and steric propensities (cone angle) of substituents R of PR₃ ligands. In a similar manner, the

* Corresponding author. Fax: +33-381-666-438.

E-mail address: michael.knorr@univ-fcomte.fr (M. Knorr).

modification of the substituent R of isocyanides CNR allows to fine-tune the σ -donor/ π -acceptor propensities of this versatile class of ligands [1–3]. In general, textbooks present both terminal and bridging isocyanides as stronger σ -donor and weaker π -acceptor ligands compared to carbon monoxide. However, Lentz has shown that fluorinated isocyanides behave also as powerful π -acceptor ligands. Especially, trifluoromethyl isocyanide is one of the strongest known π -acceptors which may excel even CO [4–7]. In the context of our interest in the coordination and activation of unsaturated organic molecules on heterobimetallic complexes $L_nM-M'L_n$, we have studied in some precedent papers the synthesis and reactivity of heterometallic couples towards isocyanides [8–14]. In the case of bis(diphenylphosphino)amine-bridged Mo–Pt and W–Pt complexes $[(OC)_4M(\mu-C=O)(\mu-dppa)Pt(PPh_3)]$, we have noticed that reaction with tosylmethyl isocyanide afforded exclusively isocyanide-bridged complexes $[(OC)_4M(\mu-C=N-CH_2SO_2p\text{-tolyl})(\mu-dppa)Pt(PPh_3)]$ (M = Mo, W), whereas treatment with xylyl isocyanide and benzyl isocyanide yielded very labile complexes $[(RNC)(OC)_3W(\mu-C=O)(\mu-dppa)Pt(PPh_3)]$ with terminal isocyanide ligands [15]. With the aim to evaluate in more detail the reasons for the different bonding mode (bridging vs. terminal), we have undertaken a study with various isocyanides having substituents R with very diverging electronic and steric features.

2. Experimental

All reactions were performed in Schlenk-tube flasks under purified nitrogen. Solvents were dried and distilled under nitrogen before use, toluene and hexane over sodium, dichloromethane from P_4O_{10} . IR spectra have been recorded on a Nicolet Nexus 470 spectrometer. Elemental C, H analyses were performed on a Leco elemental analyser CHN 900. The 1H -, $^{13}C\{^1H\}$ - and $^{31}P\{^1H\}$ -NMR spectra were recorded at 200.13, 50.32, 81.01, 63.16 and 39.76 MHz, respectively, on a Bruker ACP 200 instrument and a Bruker Avance 300 instrument (300.13 MHz for 1H). ^{195}Pt chemical shifts were measured on a Bruker ACP 200 instrument (42.95 MHz) and externally referenced to K_2PtCl_4 in water with downfield chemical shifts reported as positive. The correct analysis of the ABX spin systems listed in Table 7 has been checked by simulating the spectra using the gNMR V 3.6 software package (IvorySoft). NMR spectra were recorded in pure $CDCl_3$, unless otherwise stated. The reactions were generally monitored by IR spectroscopy in the $\nu(CO)$ region. $[M(CO)_5(\eta^1\text{-dppm})]$ (M = Cr, Mo, W), $[Pt(CH_2CH_2)(PPh_3)_2]$, $[CNCH_2PPh_3][PF_6]$ and $[CNCF_3]$ were prepared as described in the literature [16–20], the other isocyanides were obtained commercially from Fluka or Aldrich.

2.1. Preparation of $[(OC)_4Cr(\mu-CO)(\mu\text{-dppm})Pt(PPh_3)]$ (**1a**)

$[Cr(CO)_5(\eta^1\text{-dppm})]$ (1 mmol) was added to a solution of $[Pt(CH_2CH_2)(PPh_3)_2]$ (748 mg, 1 mmol) in 10 ml of toluene. The solution was stirred at 20 °C for 1 h. Ethylene evolution was observed and the solution turned rapidly to yellow–orange. After 15 min precipitation of the yellow product occurred, which was completed by slow concentration of the solution under reduced pressure and subsequent addition of hexane (10 ml). The product was filtered off, rinsed with hexane, and dried under vacuo (940 mg, 91% yield). This crude product is sufficiently pure for further reactions; analytically pure samples can be obtained by recrystallisation from concentrated CH_2Cl_2 –heptane or toluene–heptane mixtures at –25 °C. Anal. Calc. for $C_{48}H_{37}CrO_5P_3Pt \cdot CH_2Cl_2$ (1033.82 + 84.93): C, 52.60; H, 3.51. Found: C, 52.55; H, 3.65%. IR (KBr): $\nu(CO)$: 1995s, 1904sh, 1881vs, 1789m cm^{-1} . 1H -NMR: δ = 4.28 (t, PCH_2 , 2H, $^2J_{P,H}$ = 8.6, $^3J_{Pt,H}$ = 29.6 Hz), 6.85–7.55 (m, 35H, phenyl).

2.2. Preparation of $[(OC)_4Mo(\mu-CO)(\mu\text{-dppm})Pt(PPh_3)]$ (**1b**)

This complex was prepared as described for **1a** (959 mg, 89% yield). Anal. Calc. for $C_{48}H_{37}MoO_5P_3Pt$ (1077.82): C, 53.49; H, 3.46. Found: C, 53.85; H, 3.66%. IR (KBr): $\nu(CO)$: 2010s, 1914sh, 1896vs, 1800m cm^{-1} . 1H -NMR: δ = 4.25 (t, PCH_2 , 2H, $^2J_{P,H}$ = 8.5, $^3J_{Pt,H}$ = 29.0 Hz), 6.88–7.60 (m, 35H, phenyl).

2.3. Preparation of $[(OC)_4W(\mu-CO)(\mu\text{-dppm})Pt(PPh_3)]$ (**1c**)

This complex was prepared as described for **1a** (619 mg, 88% yield). Anal. Calc. for $C_{48}H_{37}O_5P_3PtW \cdot 2 CH_2Cl_2$ (1077.82 + 169.86): C, 44.97; H, 3.09. Found: C, 45.25; H, 3.05%. IR (KBr): $\nu(CO)$: 2011s, 1914sh, 1894vs, 1782m cm^{-1} . 1H -NMR: δ = 4.48 (dt, PCH_2 , 2H, $^2J_{P,H}$ = 8.8 and 1.5, $^3J_{Pt,H}$ = 34.0 Hz), 6.85–7.54 (m, 35H, phenyl).

2.4. Preparation of $[(OC)_4W(\mu\text{-CNCF}_3)(\mu\text{-dppm})Pt(PPh_3)]$ (**2**)

Compound **1c** (97 mg, 0.079 mmol) was dissolved in CH_2Cl_2 . CF_3NC (0.080 mmol) was added using ‘pVT vacuum techniques’. The solution was stirred for one hour at ambient. Afterwards *n*-pentane was added to precipitate the product in form of yellow–orange crystals, which were collected by filtration. Yield: 76%.

Anal. Calc. for $C_{49}H_{37}F_3NO_4P_3PtW$ (1232.65): C, 47.74; H, 3.03; N, 1.14. Found: C, 47.98; H, 3.09; N,

1.01%. IR (KBr): $\nu(\text{CO})$: 2021s, 1959m, 1928s, 1898vs; $\nu(\text{C}=\text{N})$ 1620m cm^{-1} . $^1\text{H-NMR}$: $\delta = 4.62$ (dt, PCH_2 , 2H, $^2J_{\text{P,H}} = 8.9$ and 1.5, $^3J_{\text{Pt,H}} = 42.0$ Hz), 6.86–7.49 (m, 35H, phenyl).

2.5. Preparation of $[(\text{OC})_4\text{Cr}(\mu\text{-CNCH}_2\text{SO}_2p\text{-tolyl})(\mu\text{-dppm})\text{Pt}(\text{PPh}_3)]$ (**3a**)

Solid *p*-tosylmethylisocyanide (98 mg, 0.5 mmol) was added in three portions to a solution of **1a** (559 mg, 0.5 mmol) in 10 ml of CH_2Cl_2 . After being stirred for 30 min, the solution was concentrated to ca. 5 ml, layered with hexane, and stored at -25°C . Yellow–orange microcrystals of **3a** were formed, which were collected after 2 days and dried under vacuo (355 mg, 59% yield). Anal. Calc. for $\text{C}_{56}\text{H}_{46}\text{CrNO}_6\text{P}_3\text{PtS}$ (1201.06): C, 56.00; H, 3.86; N, 1.17 Found: C, 55.55; H, 3.61; N, 1.04%. IR (KBr): $\nu(\text{CO})$: 1987s, 1923vs, 1890s; $\nu(\text{C}=\text{N})$ 1667m cm^{-1} . $^1\text{H-NMR}$: $\delta = 2.33$ (s, CH_3 , 3H), 4.35 (t, PCH_2 , 2H, $^2J_{\text{P,H}} = 9.4$, $^3J_{\text{Pt,H}} = 41.0$ Hz), 5.06 (s, br NCH_2 , 2H), 6.80–7.42 (m, 39H, phenyl).

2.6. Preparation of $[(\text{OC})_4\text{Mo}(\mu\text{-CNCH}_2\text{SO}_2p\text{-tolyl})(\mu\text{-dppm})\text{Pt}(\text{PPh}_3)]$ (**3b**)

This complex was prepared as described for **3a** (474 mg, 69% yield). Anal. Calc. for $\text{C}_{56}\text{H}_{46}\text{MoNO}_6\text{P}_3\text{PtS} \cdot 1.5 \text{CH}_2\text{Cl}_2$ (1201.06 + 127.39): C, 50.32; H, 3.60; N, 1.02 Found: C, 50.02; H, 3.78; N, 1.01%. IR (KBr): $\nu(\text{CO})$: 2009s, 1930sh, 1902vs; $\nu(\text{C}=\text{N})$ 1680m cm^{-1} . $^1\text{H-NMR}$: $\delta = 2.27$ (s, CH_3 , 3H), 4.26 (t, PCH_2 , 2H, $^2J_{\text{P,H}} = 9.6$, $^3J_{\text{Pt,H}} = 39.0$ Hz), 4.90 (s, br NCH_2 , 2H), 6.76–7.43 (m, 39H, phenyl).

2.7. Preparation of $[(\text{OC})_4\text{W}(\mu\text{-CNCH}_2\text{SO}_2p\text{-tolyl})(\mu\text{-dppm})\text{Pt}(\text{PPh}_3)]$ (**3c**)

This complex was prepared as described for **3a** (473 mg, 71% yield). Anal. Calc. for $\text{C}_{56}\text{H}_{46}\text{NO}_6\text{P}_3\text{PtWS}$ (1332.91): C, 50.46; H, 3.48; N, 1.05 Found: C, 50.67; H, 3.84; N, 1.07%. IR (KBr): $\nu(\text{CO})$: 2007s, 1919sh, 1894vs; $\nu(\text{C}=\text{N})$ 1654m cm^{-1} . $^1\text{H-NMR}$: $\delta = 2.37$ (s, CH_3 , 3H), 4.49 (t, PCH_2 , 2H, $^2J_{\text{P,H}} = 9.4$, $^3J_{\text{Pt,H}} = 41.0$ Hz), 4.99 (s, br NCH_2 , 2H), 6.80–7.42 (m, 39H, phenyl).

2.8. Preparation of $[(\text{OC})_4\text{W}(\mu\text{-CNCH}_2\text{PPh}_3)(\mu\text{-dppm})\text{Pt}(\text{PPh}_3)]$ [**PF**₆] (**4**)

This complex was prepared as described for **3a** (474 mg, 61% yield). Anal. Calc. for $\text{C}_{67}\text{H}_{54}\text{NO}_4\text{P}_3\text{PtW} \cdot \text{PF}_6$ (1554.01): C, 51.79; H, 3.50; N, 0.90 Found: C, 51.39; H, 3.31; N, 0.84%. IR (KBr): $\nu(\text{CO})$: 2011s, 1929s, 1896vs; $\nu(\text{C}=\text{N})$ 1622m cm^{-1} . $^1\text{H-NMR}$: $\delta = 4.61$ (dt, PCH_2 , 2H, $^2J_{\text{P,H}} = 9.2$ and 1.5, $^3J_{\text{Pt,H}} = 27.5$ Hz), 5.13 (m, 2H, NCH_2), 6.86–7.49 (m, 50H, phenyl).

2.9. Preparation of $[(\text{benzylNC})(\text{OC})_3\text{W}(\mu\text{-CO})(\mu\text{-dppm})\text{Pt}(\text{PPh}_3)]$ (**5**) and of *cis*- $[(\text{benzylNC})(\text{OC})_4\text{W}(\eta^1\text{-dppm})]$ (**8a**)

Complex **5** was prepared as described for **3a** and isolated as orange–red powder. Since the crude product contained ca. 10% of **8a** as impurity, no correct elemental analysis could be obtained. IR (CH_2Cl_2): $\nu(\text{CN})$ 2148m; $\nu(\text{CO})$: 2014s, 1920sh, 1902vs; $\nu(\text{C}=\text{O})$ 1786m cm^{-1} . $^1\text{H-NMR}$: $\delta = 4.45$ (t, PCH_2 , 2H, $^2J_{\text{P,H}} = 9.2$ Hz), 5.13 (m, 2H, NCH_2), 6.86–7.49 (m, 40H, phenyl). During attempts of purification, further fragmentation occurred. Among the degradation products, yellow air-stable **8a** co-crystallized. Suitable crystals for X-ray diffraction were grown from CHCl_3 –heptane. Anal. Calc. for $\text{C}_{37}\text{H}_{29}\text{NO}_4\text{P}_2\text{W}$ (797.44): C, 55.73; H, 3.66; N, 1.76 Found: C, 54.79; H, 3.79; N, 1.83%. IR (CH_2Cl_2): $\nu(\text{CN})$ 2147m; $\nu(\text{CO})$: 2012s, 1931s, 1906vs cm^{-1} . $^1\text{H-NMR}$: $\delta = 3.27$ (dd, PCH_2 , 2H, $^2J_{\text{P,H}} = 7.5$ and 1.2 Hz), 4.34 (m, 2H, NCH_2), 6.88–7.38 (m, 25H, phenyl). $^{13}\text{C}\{^1\text{H}\}$ -NMR: $\delta = 47.3$ (t, PCH_2 , $^1J_{\text{P,C}} = 37$ Hz), 138.3 (s, vbr, CH_2), 152.7 (s, vbr, CN), 199.8 (dd, 2CO_{cis} , $^2J_{\text{P,C}} = 7$, $^4J_{\text{P,C}} = 2$ Hz), 202.6 (dd, 1CO_{cis} , $^2J_{\text{P,C}} = 6$, $^4J_{\text{P,C}} = 2$ Hz), 203.9 (d, $1\text{CO}_{\text{trans}}$, $^2J_{\text{P,C}} = 25$ Hz).

2.10. Preparation of $[(\text{cyclohexylNC})(\text{OC})_3\text{W}(\mu\text{-CO})(\mu\text{-dppm})\text{Pt}(\text{PPh}_3)]$ (**6**) and of *cis*- $[(\text{cyclohexylNC})(\text{OC})_4\text{W}(\eta^1\text{-dppm})]$ (**8b**)

Complex **6** was prepared as described for **5** and isolated as an orange–red powder. Since the crude product contained ca. 20% of **8b** as impurity, no correct elemental analysis could be obtained. IR (CH_2Cl_2): $\nu(\text{CN})$ 2144m; $\nu(\text{CO})$: 2013s, 1901vs, 1882sh; $\nu(\text{C}=\text{O})$ 1792m cm^{-1} . $^1\text{H-NMR}$: $\delta = 1.28$ –1.62 (m, 11H, C_6H_{11}), 4.52 (t, PCH_2 , 2H, $^2J_{\text{P,H}} = 8.4$, $^3J_{\text{Pt,H}} = 32$ Hz), 6.86–7.49 (m, 50H, phenyl).

Compound **8b**: IR (CH_2Cl_2): $\nu(\text{CN})$ 2144m; $\nu(\text{CO})$: 2013s, 1931s, 1906vs cm^{-1} . $^1\text{H-NMR}$: $\delta = 1.29$ –1.61 (m, 11H, C_6H_{11}), 3.33 (dd, PCH_2 , 2H, $^2J_{\text{P,H}} = 7.3$ and 1.2 Hz), 6.90–7.68 (m, 20H, phenyl).

2.11. Preparation of $[(\text{OC})_3\text{Fe}\{\mu\text{-C}=\text{N}-\text{CH}_2\text{PO}(\text{OEt})_2\}(\mu\text{-dppm})\text{Pt}(\text{PPh}_3)]$ (**9**)

To a solution of $[(\text{OC})_3\text{Fe}(\mu\text{-CO})(\mu\text{-dppm})\text{Pt}(\text{PPh}_3)]$ (505 mg, 0.5 mmol) in 10 ml of dichloromethane was added dropwise $\text{CNCH}_2\text{PO}(\text{OEt})_2$ (80 μl , 0.5 mmol) by means of a micro-syringe. The orange reaction mixture was stirred at room temperature for 30 min and then concentrated to ca. 4ml under reduced pressure. Addition of a hexane layer gave after 2 days in a refrigerator large orange crystals solvated with dichloromethane (478 mg, 77% yield). Anal. Calc. for $\text{C}_{52}\text{H}_{49}\text{FeNO}_6\text{P}_4\text{Pt} \cdot \text{CH}_2\text{Cl}_2$ (1158.79 + 84.93): C, 51.18;

H 4.13; N, 1.13. Found: C, 50.98; H 4.55; N, 1.24%. IR (KBr): $\nu(\text{CO})$: 1994s, 1923vs, 1904sh; $\nu(\text{C}=\text{N})$ 1648m cm^{-1} . $^1\text{H-NMR}$: $\delta = 1.07$ (t, CH_3 , 6H, $^2J_{\text{H,H}} = 7.0$ Hz), 3.85 (m, OCH_2 , 4H and PCH_2 , 2H), 4.22 (d, NCH_2 , 2H, $^2J_{\text{P,H}} = 13.1$ Hz), 7.11–7.35 (m, 35H, phenyl).

2.12. Preparation of $[(\text{OC})_4\text{W}(\mu\text{-C}=\text{N}(\text{H})\text{CF}_3)(\mu\text{-dppm})\text{Pt}(\text{PPh}_3)][\text{BF}_4]$ (**10**)

To a solution of **2** (10 mg) in 2 ml of dichloromethane was added a drop of $\text{HBF}_4 \cdot \text{Et}_2\text{O}$. All volatiles were removed under vacuo. NMR examination of the yellow residue indicated quantitative formation of **10**. The FAB^+ mass spectrum (NBA matrix) exhibits with 100% intensity the peak for the cation at m/z 1234, whose experimental isotope distribution pattern matches with the simulated one. IR (KBr): $\nu(\text{CO})$: 2062s, 1981m, 1944vs cm^{-1} . $^1\text{H-NMR}$: $\delta = 5.30$ (t, PCH_2 , 2H, $^2J_{\text{P,H}} = 10.0$, $^3J_{\text{Pt,H}} = 24.0$ Hz), 6.50–7.65 (m, 35H, phenyl), 8.45 (m, br, CNH , 1H).

2.13. Preparation of $[(\text{OC})_4\text{Mo}(\mu\text{-C}=\text{N}(\text{H})\text{CH}_2\text{SO}_2\text{p-tolyl})(\mu\text{-dppm})\text{Pt}(\text{PPh}_3)][\text{BF}_4]$ (**11**)

This complex was prepared by addition of an excess of $\text{HBF}_4 \cdot \text{Et}_2\text{O}$ at 253 K to a solution of **3b** (125 mg, 0.1 mmol) in CH_2Cl_2 (5 ml). After stirring for 10 min, all volatiles were removed under reduced pressure. The yellow residue was rinsed with Et_2O (2ml) and then dried under vacuo (133 mg, 94% yield). Anal. Calc. for $\text{C}_{56}\text{H}_{47}\text{MoNO}_6\text{P}_3\text{PtBF}_4 \cdot \text{CH}_2\text{Cl}_2$ (1332.81 + 84.93): C, 48.29; H 3.48; N, 0.99. Found: C, 48.56; H 3.68; N, 1.06%. IR (CH_2Cl_2): $\nu(\text{CO})$: 2051s, 2005m, 1946vs cm^{-1} . $^1\text{H-NMR}$: $\delta = 2.41$ (s, CH_3 , 3H), 4.73 (t, PCH_2 , 2H, $^2J_{\text{P,H}} = 10.0$, $^3J_{\text{Pt,H}} = 21.0$ Hz), 4.95 (d, NCH_2 , 2H, $^3J_{\text{P,H}} = 5.9$ Hz), 6.6–7.65 (m, 39H, phenyl), 8.16 (m, br, CNH , 1H).

2.14. Crystal structure determinations

A crystal of compound **2** was mounted on the top of a glass fibre and brought immediately into the cold gas stream of a Bruker-AXS Smart 1000 diffractometer. Data of **2** were collected at 153(2) K. A total of 4200 frames were recorded by ω -scans ($\Delta\omega = 0.3^\circ$, 30 s) at seven different ϕ positions. The intensities were determined and corrected by the program SAINT (area-detector integration software; Siemens Industrial Automation Inc., Madison, WI, 1995). An empirical absorption correction (SADABS, area-detector absorption correction; Siemens Industrial Automation Inc., Madison, WI, 1996) was employed using the multiscan method [21]. Data of **3c** and **9** were collected on a Siemens AED2 diffractometer using graphite-monochromated Mo-K_α radiation ($\lambda = 0.71069 \text{ \AA}$). The intensities were collected using Ω - 2θ scans, and the

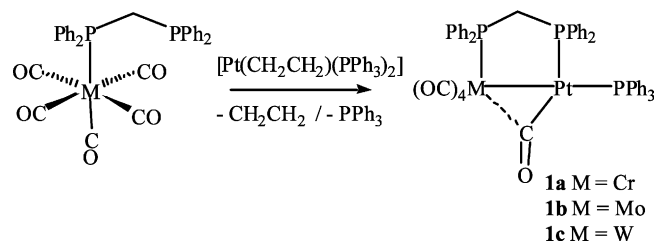
intensities of three standard reflections, which were measured after every 100 reflections, remained stable throughout each data collection. The intensities were corrected for Lorentz and polarization effects. An empirical absorption correction based on the Ψ -scans of three reflections was employed. Data of **1a,c** and **8a** were collected on a Stoe IPDS diffractometer. The intensities were determined and corrected by the program INTEGRATE in IPDS (Stoe & Cie, 1999). An empirical absorption correction was employed using the FACEIT-program in IPDS (Stoe & Cie, 1999).

The structures were generally solved by direct and Fourier methods using SHELXS-97. For each structure, the non-hydrogen atoms were refined anisotropically. All of the H-atoms were placed in geometrically calculated positions and each was assigned a fixed isotropic displacement parameter based on a riding-model. Refinement of the structures was carried out by full-matrix least-squares methods based on F_o^2 using SHELXL-97. All calculations were performed using the WINGX crystallographic software package, using the programs SHELXS-97 and SHELXL-97 [22]. The crystallographic data for each complex are given in Table 8.

3. Results and discussion

3.1. Syntheses and characterisation of $[(\text{OC})_4\text{M}(\mu\text{-C}=\text{O})(\mu\text{-dppm})\text{Pt}(\text{PPh}_3)]$

In order to evaluate also the influence of the bridging diphosphane backbone on the outcome of the reaction of $[(\text{OC})_4\text{M}(\mu\text{-C}=\text{O})(\mu\text{-Ph}_2\text{PXPPh}_2)\text{Pt}(\text{PPh}_3)]$ ($\text{X} = \text{NH}$, CH_2) with CNR, we have chosen dppm as diphosphane backbone. This ligand is known to be more electron-donating compared to dppe (see below). To allow a comparison with some recently prepared Fe–Pt isocyanide complexes, we furthermore extended our study to Cr–Pt complexes. The hitherto unknown complexes $[(\text{OC})_4\text{M}(\mu\text{-C}=\text{O})(\mu\text{-dppm})\text{Pt}(\text{PPh}_3)]$ (**1a–c**) were obtained by reaction of $[\text{M}(\text{CO})_5(\eta^1\text{-dppm})]$ ($\text{M} = \text{Cr}$, Mo , W) with $[\text{Pt}(\text{CH}_2\text{CH}_2)(\text{PPh}_3)_2]$ in toluene with 70–85% yield. The yellow–orange compounds, which are insoluble in hexane or Et_2O , are air stable as solids but gradually decompose in halogenated solvents (Scheme 1).



Scheme 1.

3.1.1. Spectroscopic data

The $^{31}\text{P}\{^1\text{H}\}$ -NMR spectra of **1a–c** consist of three mutually coupled doublet of doublets (Table 7). Whereas in the case of **1a** the three resonances at δ 55.9 (P^1Cr), 45.1 (PPh_3Pt) and 10.1 (P^2Pt) are quite distinct, the resonances of P^1 and P^2 approach in the case of **1b** and give finally rise to an ABX spin system in the case of **1c**, the AB part being centred at δ 13.0 ppm. The chemical shift of the Pt signal in the $^{195}\text{Pt}\{^1\text{H}\}$ -NMR spectra of **1a–c** is not much affected by the nature of the adjacent metal centre (δ **1a** –2431.5, **1b** –2514.5, **1c** –2484.0). In the case of **1b,c** the signal is splitted in the expected doublet of doublet of doublets pattern due a coupling with three phosphorous nuclei, whereas in the case of **1a** (and **3a**) the $^{2+3}J_{\text{Pt,P}}$ coupling is probably too weak to be observed. The IR spectra of **1a–c** show in addition to three terminal $\nu(\text{CO})$ stretches a vibration at 1789 (**1a**), 1800 (**1b**) and 1781 (**1c**) cm^{-1} for a (semi)bridging carbonyl ligand. These positions are between those found for genuine $\mu(\text{CO})$ vibrations (e.g. $[(\text{OC})_3\text{Fe}(\mu\text{-C=O})(\mu\text{-dppm})\text{Pt}(\text{PPh}_3)]$ 1760 cm^{-1}) [23] and typical semi-bridging vibrations (e.g. $[(\text{Me}_3\text{P})(\text{OC})_4\text{Cr}(\mu\text{-CPh})\text{Pt}(\text{PMe}_3)_2][\text{BF}_4]$ 1833 cm^{-1} ; $[\text{Cp}(\text{OC})_3\text{MoPt}(\text{H})(\text{PPh}_3)_2]$ 1820 cm^{-1} ; $[\text{Cp}(\text{OC})_2\text{W}(\mu\text{-dppm})\text{Pt}(\eta^1\text{-dppm})][\text{PF}_6]$ 1797 cm^{-1}). [24,25a,b] The molecular structures of **1a** and **1c** have been determined to (i) clarify the kind of bridging interaction between M and Pt and (ii) to allow a structural comparison of the CO-bridged starting materials with their $\mu\text{-CNR}$ counterparts (see below).

3.1.2. Crystal structures of $[(\text{OC})_4\text{M}(\mu\text{-C=O})(\mu\text{-dppm})\text{Pt}(\text{PPh}_3)]$ (**1a** and **1c**)

Suitable crystals of **1a** and **1c** for an X-ray diffraction study were grown from toluene/heptane and CH_2Cl_2 -heptane, respectively. The molecular structures are depicted in Figs. 1 and 2a,b, selected bond lengths and angles are given in Tables 1 and 2. The coordination around chromium of **1a** is best described as distorted octahedral with an additional metal–metal bond bisecting the angle between C(4) and C(5), thus being seven-coordinate. The Cr–Pt distance of 277.49(8) pm lies half-way between that reported for $[(\text{Me}_3\text{P})(\text{OC})_3\text{Cr}(\mu\text{-C=O})\{\mu\text{-C}(\text{CO}_2\text{Me})\}\text{Pt}(\text{PMe}_3)_2]$ [266.6(7) pm] and $[(\text{OC})_4\text{Cr}(\mu\text{-C=O})(\mu\text{-PPh}_2)\text{Pt}(\eta^3\text{-cyclooctenyl})]$ [282.0(1) pm] [24,26]. The two metal centres are spanned by the diphosphane-ligand forming a distorted five-membered ring with a torsion angle $\text{P}(1)\text{–Cr–Pt–P}(2)$ of 34.4° . In addition, the Cr–Pt bond is bridged asymmetrically by a carbonyl ligand with very long Cr–C(1) bond [238.9(4) pm] and a short Pt–C(1) bond [190.4(4) pm]. This semi(bridging) bonding situation needs some comment: compared with Shaw's compound $[(\text{OC})_3\text{Fe}(\mu\text{-C=O})(\mu\text{-dppm})\text{Pt}(\text{PPh}_3)]$ [27] (the van der Waals radii of Cr and Fe are approximately comparable) possessing a symmetrically bridging $\mu\text{-CO}$ ligand [Fe– $\mu\text{-C}$ 201.2(7) pm; Pt–

$\mu\text{-C}$ 199.2(7) pm], the asymmetry of **1a** with angles Cr–C(1)–O(1) and Pt–C(1)–O(1) of $128.1(3)$ and $152.0(3)^\circ$ is evident. The above mentioned compounds $[(\text{Me}_3\text{P})(\text{OC})_3\text{Cr}(\mu\text{-C=O})\{\mu\text{-C}(\text{CO}_2\text{Me})\}\text{Pt}(\text{PMe}_3)_2]$ and $[(\text{OC})_4\text{Cr}(\mu\text{-C=O})(\mu\text{-PPh}_2)\text{Pt}(\eta^3\text{-cyclooctenyl})]$ possess also asymmetric bridging carbonyls, but in both cases the Pt– $\mu\text{-C}$ bonds are significantly longer [219.3(0) and 225.2(7) pm] than the Cr– $\mu\text{-C}$ bonds [175.0(5) and 197.6(7) pm] (Chart 1).

The ligand arrangement of **1c** is very similar to that of **1a**. The adjacent metals are connected via W–Pt bond, the distance of 287.6(3) pm being quite close to that of $[(\text{HBpz}_3)(\text{OC})\text{W}(\mu\text{-C=O})\{\mu\text{-}\eta^1\text{-}\eta^2\text{-C}(\text{H})(\text{NET}_2)\}\text{Pt}(\text{PEt}_3)_2][\text{BF}_4]$ [287.1(10) pm] and $[(\text{PPh}_3)(\text{OC})_3\text{W}(\mu\text{-C=O})\{\mu\text{-P}(\text{Ph})(\text{C}_5\text{H}_4\text{C}_5\text{H}_4)\}\text{Pt}(\text{PPh}_3)]$ [291.56(1) pm] [28,29]. Again, a carbonyl ligand bridges in an asymmetric manner the metal–metal bond. In spite of the very similar atomic radii of W and Pt (1.30 Å), the W–C(1) distance [241.8(8) pm] is significantly longer than the corresponding Pt–C(1) distance [192.3(10) pm] (Fig. 2a,b). This contrasts again with the (semi)bridging CO bonding mode reported for $[(\text{HBpz}_3)(\text{OC})\text{W}(\mu\text{-C=O})\{\mu\text{-}\eta^1\text{-}\eta^2\text{-C}(\text{H})(\text{NET}_2)\}\text{Pt}(\text{PEt}_3)_2][\text{BF}_4]$ and $[(\text{PPh}_3)(\text{OC})_3\text{W}(\mu\text{-C=O})\{\mu\text{-P}(\text{Ph})(\text{C}_5\text{H}_4\text{C}_5\text{H}_4)\}\text{Pt}(\text{PPh}_3)]$, where the Pt– $\mu\text{-C}$ bonds are by far longer [228.0(2) and 243.1(3) pm] than the W– $\mu\text{-C}$ bonds [208.0(4) and 202.0(3) pm]. [28,29] In the case of the dppm-spanned compound $[\text{Cp}(\text{OC})_2\text{W}(\mu\text{-dppm})\text{Pt}(\eta^1\text{-dppm})][\text{PF}_6]$ [d W–Pt 290.2(2) pm] possessing a slightly semi-bridging carbonyl, the Pt– $\mu\text{-C}$ contact is still weaker [261.2(2) pm]. [25b] At present, we are however unable to give a rationalisation for the structural features of compounds **1**, some future theoretical calculations seem necessary for an understanding of the electronic structure of these heterometallic systems.

3.2. Syntheses and characterisation of $[(\text{OC})_4\text{M}(\mu\text{-C=N-R})(\mu\text{-dppm})\text{Pt}(\text{PPh}_3)]$

The reaction of **1c** in dichloromethane at ambient temperature with the strong π -accepting isocyanides CNCF_3 , $\text{CNCH}_2\text{SO}_2p\text{-tolyl}$ and $[\text{CNCH}_2\text{PPh}_3][\text{PF}_6]$ gave within 10 min exclusively the bright yellow complexes $[(\text{OC})_4\text{W}(\mu\text{-C=N-R})(\mu\text{-dppm})\text{Pt}(\text{PPh}_3)]$ (**2**, **3c** and **4**) by substitution of the bridging carbonyl ligand according Scheme 2. In similar manner, the orange–yellow compounds $[(\text{OC})_4\text{Cr}(\mu\text{-C=N-CH}_2\text{SO}_2p\text{-tolyl})(\mu\text{-dppm})\text{Pt}(\text{PPh}_3)]$ (**3a**) and $[(\text{OC})_4\text{Mo}(\mu\text{-C=N-CH}_2\text{SO}_2p\text{-tolyl})(\mu\text{-dppm})\text{Pt}(\text{PPh}_3)]$ (**3b**) were formed

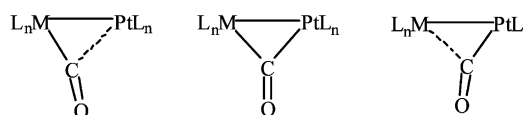


Chart 1.

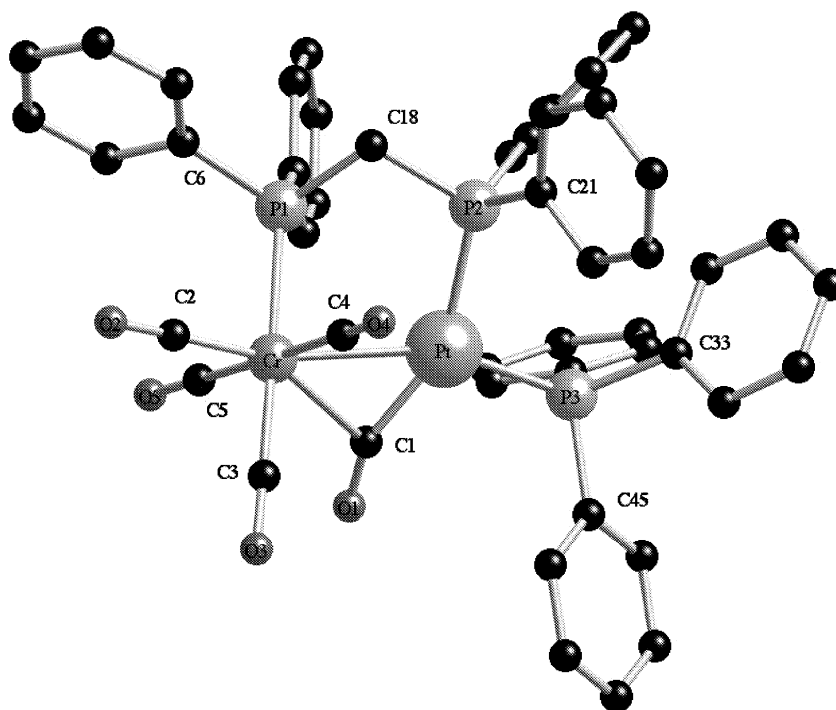
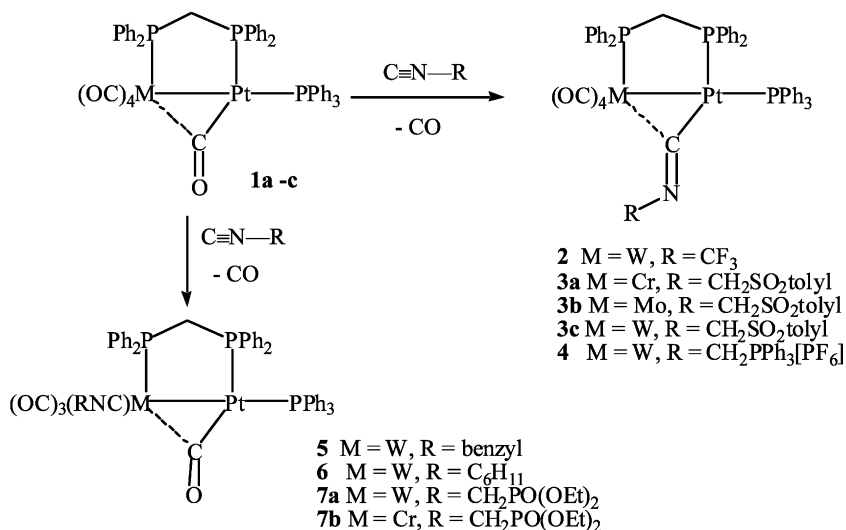


Fig. 1. View of the molecular structure of **1a** with the numbering scheme.

upon stoichiometric treatment of **1a,b** with tosylmethylisocyanide. All derivatives are stable as solids at least for some weeks, but gradually decompose in halogenated solvents. Again, the three phosphorous nuclei of W–Pt core give rise to ABX spin systems in the ^{31}P -NMR spectra (Table 7). In addition, each of the 4 visible lines of the X-part of **2** are further splitted into a quadruplet due to a weak $^5J_{\text{P,F}}$ coupling with the CF_3 substituent. The stronger donor character of dppm compared with dppa can be inferred from the IR spectra, since the position of the carbonyl bands of **3b,c** is shifted approximately 10 wave-numbers to lower

frequencies with respect to their dppa-counterparts. Indicative for the bridging bonding mode of the CNR ligand is the presence of a $\nu(\text{C}=\text{N})$ vibration of medium intensity in the range between $1620\text{--}1680\text{ cm}^{-1}$. Within the series **3a–c**, the position of this vibration is quite close in the case of the Cr–Pt and Mo–Pt derivatives (1672 vs. 1679 cm^{-1}), but is shifted to lower wave numbers for the W–Pt analogue (1655 cm^{-1}). The particular low frequency in the case of **2** compared to **3c** (1620 vs. 1655 cm^{-1}) is coherent with the elongation of the C=N bond length observed in the crystal structures of those complexes (see below).



Scheme 2.

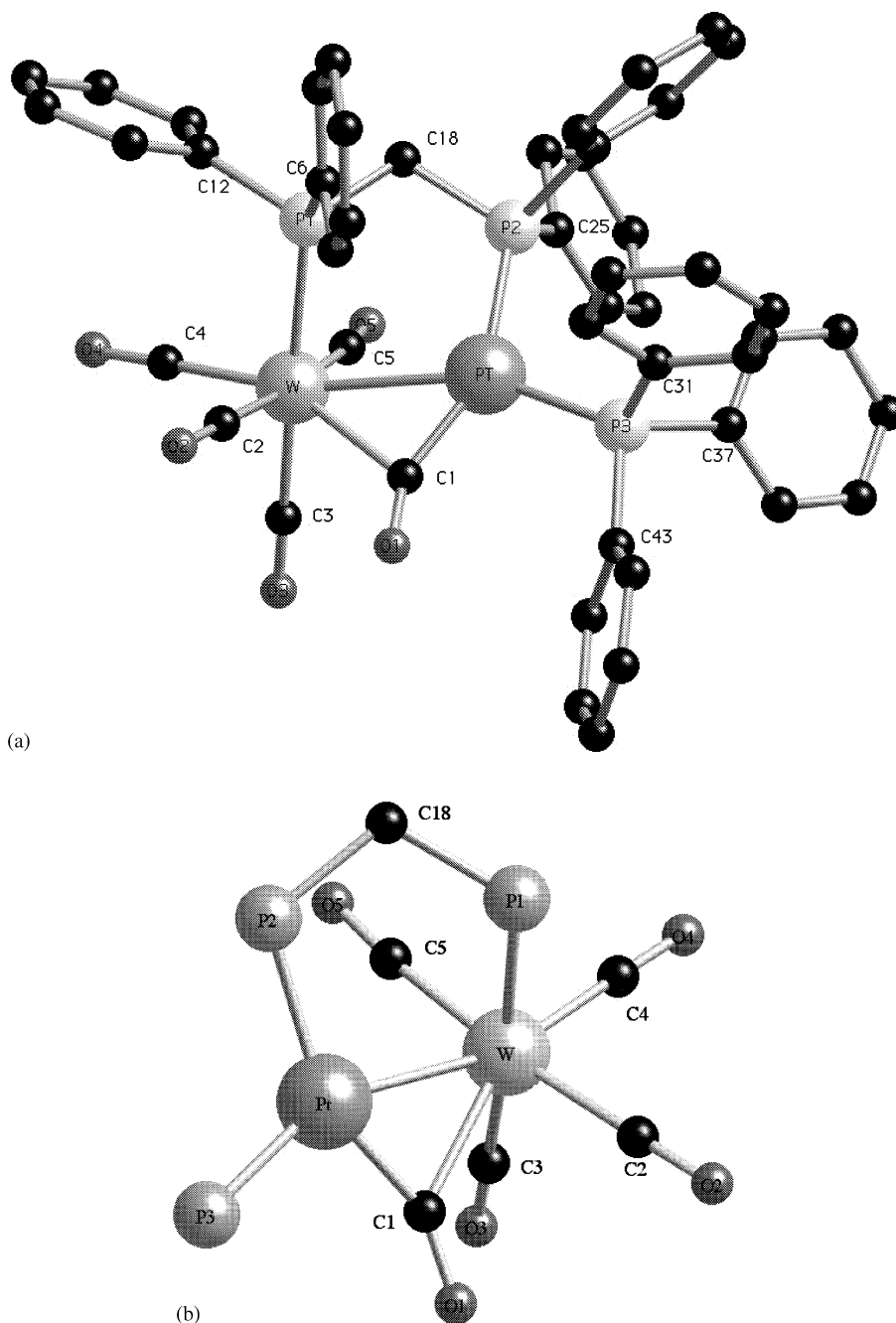


Fig. 2. (a) View of the molecular structure of **1c** with the numbering scheme. (b) Perspective view of the core structure of **1c** along the Pt–W bond. The phenyl groups are omitted for clarity.

3.2.1. Crystal structures of $[(OC)_4W(\mu-C=N-R)(\mu-dppm)Pt(PPh_3)]$ (**2** and **3c**)

Suitable crystals of **2** for an X-ray diffraction study were grown from CH_2Cl_2 –heptane at $-30^\circ C$. The molecular structure is depicted in Fig. 3, selected bond lengths and angles are given in Table 3. The overall geometries of **2** and **3c** are quite related to that of their precursor **1c**. Thus, the coordination around the tungsten centre of **2** is also seven-coordinate due to presence of a W–Pt bond. The W–Pt distance of 279.07(4) pm has however significantly shrunk about 8 pm compared

to that of **1c** and parallels that reported for $[(OC)_5W(\mu-C=CH_2)Pt(dppm)]$ [277.4(1) pm] [30]. The torsion angle P(1)–W–Pt–P(2) of the five-membered ring formed with the dppm-backbone is less distorted (34.25°) than that of **1c** (39.15°). As for **1c**, the W–Pt bond is bridged asymmetrically by the organic ligand by a long W– μ -C bond and a short Pt– μ -C bond. The degree of asymmetry is, however, less pronounced, since the W–C(1) distance is now remarkably shorter [225.4(4) vs. 241.8(8) pm], whereas the Pt–C(1) separation has increased by ca. 5 pm [196.9(4) vs. 192.3(10) pm]. Compared with the

Table 1
Selected bond lengths (pm) and bond angles (°) for **1a**

Bond lengths			
Cr–Pt	277.49(8)	Cr–C(2)	184.2(4)
Pt–P(3)	229.73(9)	Cr–C(3)	186.1(4)
Pt–P(2)	233.49(12)	Cr–C(4)	190.8(4)
Pt–C(1)	190.4(4)	Cr–C(5)	188.2(4)
Cr–P(1)	238.36(12)	C(1)–O(1)	118.2(5)
Cr–C(1)	238.9(4)		
Bond angles			
C(2)–Cr–C(5)	88.46(17)	P(2)–Pt–P(3)	104.34(4)
P(1)–C(18)–P(2)	107.35(18)	Pt–C(1)–Cr	79.66(14)
P(1)–Cr–C(2)	89.82(11)	Pt–Cr–C(1)	42.46(10)
P(1)–Cr–C(3)	178.28(13)	C(1)–Cr–C(5)	77.93(15)
P(1)–Cr–C(1)	109.08(10)	C(3)–Cr–C(1)	72.62(15)
P(1)–Cr–C(4)	89.94(11)	C(2)–Cr–C(3)	88.60(16)
P(1)–Cr–C(5)	89.86(11)	C(3)–Cr–C(5)	90.78(17)
Cr–Pt–P(3)	157.83(3)	C(2)–Cr–C(4)	89.40(17)
Cr–Pt–P(2)	97.82(3)	C(3)–Cr–C(4)	89.36(17)
P(1)–Cr–Pt	79.19(3)	C(1)–Cr–C(4)	177.86(16)
Pt–C(5)–O(5)	152.0(3)	C(2)–Cr–C(5)	156.42(16)
Cr–C(5)–O(5)	128.1(3)		

Table 2
Selected bond lengths (pm) and bond angles (°) for **1c**

Bond lengths			
W–Pt	287.6(3)	W–C(2)	205.1(9)
Pt–P(3)	229.9(4)	W–C(3)	199.0(10)
Pt–P(2)	233.6(3)	W–C(4)	198.7(9)
Pt–C(1)	192.3(1)	W–C(5)	203.8(10)
W–P(1)	250.2(3)	C(1)–O(1)	117.8(11)
W–C(1)	241.8(8)		
Bond angles			
C(2)–W–C(1)	75.2(3)	P(2)–Pt–P(3)	108.85(11)
P(1)–C(18)–P(2)	111.2(4)	Pt–C(1)–W	82.1(3)
P(1)–W–C(2)	93.9(3)	Pt–W–C(1)	41.5(2)
P(1)–W–C(3)	173.3(3)	C(1)–W–C(5)	111.5(3)
P(1)–W–C(4)	90.2(3)	C(3)–W–C(5)	87.4(4)
P(1)–W–C(1)	108.1(3)	C(2)–W–C(3)	92.4(4)
P(1)–W–C(5)	86.1(3)	C(3)–W–C(1)	75.7(3)
W–Pt–P(3)	155.21(7)	C(2)–W–C(4)	85.7(4)
W–Pt–P(2)	95.93(10)	C(3)–W–C(4)	88.1(4)
P(1)–W–Pt	77.61(10)	C(1)–W–C(4)	154.1(4)
Pt–C(1)–O(1)	149.8(7)	C(2)–W–C(5)	172.9(3)
W–C(1)–O(1)	128.0(7)		

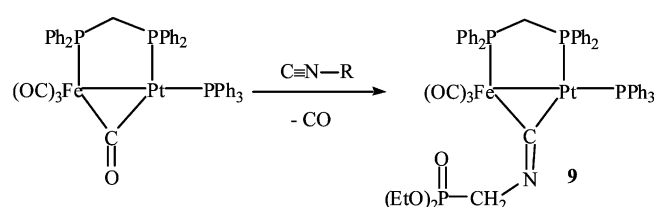
lengths of the C(1)–N double bond of **3c**, the C(1)–N double bond of **2** is somewhat longer [123.9(9) vs. 124.7(5) pm]. This lengthening is probably based on the stronger electron-withdrawing propensity of CF₃ compared to CH₂–tosyl, consistent with the excellent π -acceptor behaviour of CNCF₃ based on back-bonding into its π^* orbitals. A comparable lengths of the C=N bond [124.0(3) pm] has been encountered in the trinuclear cluster [Os₃(CO)₁₀(μ -C=N–CF₃)]. [31] As already observed for [(OC)₄W(μ -C=N–tosyl)(μ -dppa)Pt(PPh₃)], the C(1)–N–C(2) angle is strongly bent [128.5(4)°], the C(1)–N–CF₃ unit being aligned

parallel to the W–Pt axis. The Pt atom is present in a distorted square planar environment, the root mean square deviation from the plane defined by Pt, W, P(2), P(3) and C(1) being 0.055 Å. An electronic description for the bimetallic system consisting in a 18-electron count for the tungsten centre and a 16-electron configuration for the Pt⁰ centre seems appropriate. The molecular structure of **3c** (see Fig. 4 and Table 4) corresponds to that reported for [(OC)₄W(μ -C=N–CH₂SO₂*p*-tolyl)(μ -dppa)Pt(PPh₃)] and deserves no further comments. [15] The separation of the two metal centres of 283.87(6) pm is somewhat more important than that of its dppa-bridged analogue [281.0(2) pm] and that of **2**, but inferior to that of **1c**.

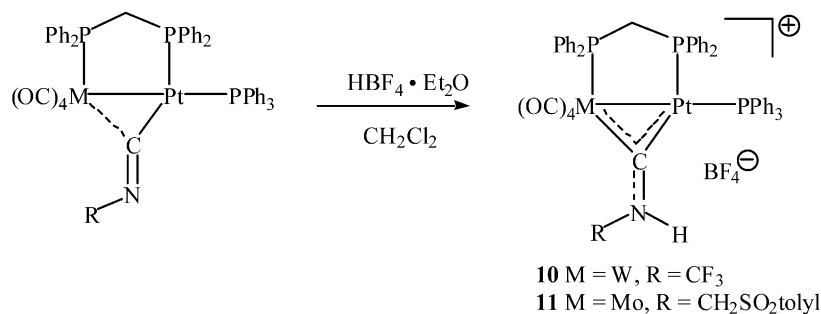
3.3. Syntheses and characterisation of [(OC)₃(RNC)M(μ -CO)(μ -dppm)Pt(PPh₃)]

The site selectivity of the carbonyl substitution by CNR seems to depend in a very sensitive manner on the nucleophilic character of the isocyanide ligand. Upon stoichiometric reaction of **1c** with benzyliocyanide, exclusively the complex [(BzNC)(OC)₃W(μ -C=O)(μ -dppm)Pt(PPh₃)] (**5**) ligated by a terminal isonitrile on tungsten is formed according the IR and NMR data. The conservation of the bridging carbonyl is evidenced by the observation of a μ (C=O) stretch at 1786 cm⁻¹, the presence of an terminal isocyanide ligand is indicated by a μ (C≡N) stretch of medium intensity at 2148 cm⁻¹. Chemical shifts and coupling constants of the ABX system in the ³¹Pt{¹H}-NMR and the doublet of doublets pattern in the ¹⁹⁵Pt{¹H}-NMR spectra are quite close to that of the precursor **1c**. The outcome of the reaction with cyclohexyl isocyanide is identical (Scheme 2). Even with diethyl(isocyanomethyl)phosphonate, which can not be considered as strong nucleophilic isocyanide, the terminal bonding mode of CNCH₂PO(OEt)₂ is encountered giving [(EtO)₂OPCH₂NC}(OC)₃W(μ -C=O)(μ -dppm)Pt(PPh₃)] (**7a**).

Unfortunately, the stability of **5–7** in solution is limited due to progressive fragmentation into mono-nuclear fragments. Therefore, no single crystals for X-ray diffraction studies or correct elemental analyses could be obtained. However, the formation of **7a** was furthermore ascertained by a FAB⁺ mass spectrum of the crude product displaying a peak at *m/z* 1314 with



Scheme 3.



Scheme 4.

24% intensity, whose experimental isotope distribution pattern matched well with the simulated one. Among the mononuclear fragments formed during the degradation, the metallophosphine *cis*-[(benzylNC)(OC)₄W(η¹-dppm)] (**8a**) crystallized during attempts of recrystallisation of **5**. Formation of *cis*-[(cyclohexylNC)(OC)₄W(η¹-dppm)] (**8b**) was also observed during the synthesis of **6**. The yellow–orange complex **8a** was completely characterized by multinuclear NMR and IR spectroscopy. In addition, the *cis*-arrangement between P(1) and C(5) of the linear isocyanide ligand [C(5)–N–C(6) 179.0(2)°] was confirmed by an X-ray diffraction study (Fig. 5). Further selected bond length and angles of this octahe-

dral complex, whose overall structure is comparable with that of [(OC)₅W(η¹-dppm)] [18] are given in Table 5.

3.4. Syntheses and characterisation of [(OC)₃Fe{μ-C=N-CH₂PO(OEt)₂}(μ-dppm)Pt(PPh₃)]

For comparison, we reacted also [(OC)₃Fe(μ-C=O)(μ-dppm)Pt(PPh₃)] with CNCH₂PO(OEt)₂ in dichloromethane at ambient temperature (Scheme 3). It seems that the Fe–Pt system is much more insensitive with respect to the electronic properties of the CNR ligand, since in contrast to **6**, the isocyanide ligand of

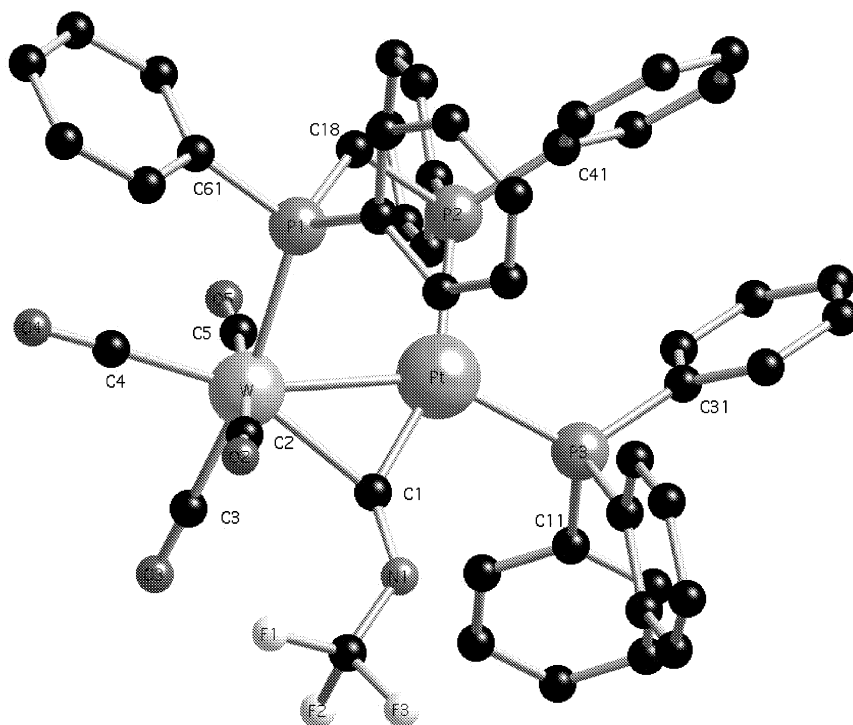
Fig. 3. View of the molecular structure of **2** with the numbering scheme.

Table 3
Selected bond lengths (pm) and bond angles (°) for **2**

<i>Bond lengths</i>			
W–Pt	279.07(4)	W–C(2)	202.3(5)
Pt–P(3)	226.98(11)	W–C(3)	199.6(6)
Pt–P(2)	231.74(11)	W–C(4)	200.0(5)
Pt–C(1)	196.9(4)	W–C(5)	205.0(6)
W–P(1)	251.20(11)	C(1)–N	124.7(5)
W–C(1)	225.4(4)		
<i>Bond angles</i>			
C(2)–W–C(1)	81.92(16)	P(2)–Pt–P(3)	108.93(4)
P(1)–C(18)–P(2)	110.6(2)	Pt–C(1)–W	82.43(15)
P(1)–W–C(2)	88.28(13)	Pt–W–C(1)	44.39(10)
P(1)–W–C(3)	170.79(17)	C(1)–W–C(5)	104.53(18)
P(1)–W–C(4)	87.88(16)	C(3)–W–C(5)	86.8(2)
P(1)–W–C(1)	111.40(10)	C(2)–W–C(3)	96.2(2)
P(1)–W–C(5)	87.98(15)	C(3)–W–C(1)	77.30(19)
W–Pt–P(3)	148.99(3)	C(2)–W–C(4)	87.1(2)
W–Pt–P(2)	102.01(3)	C(3)–W–C(4)	84.3(42)
P(1)–W–Pt	76.71(2)	C(1)–W–C(4)	157.35(19)
Pt–C(1)–N	132.8(3)	C(1)–N–C(2)	128.5(4)
W–C(1)–N	144.8(3)		

Table 4
Selected bond lengths (pm) and bond angles (°) for **3c**

<i>Bond lengths</i>			
W–Pt	283.87(6)	W–C(10)	199.3(10)
Pt–P(3)	227.89(19)	W–C(11)	201.5(9)
Pt–P(2)	232.04(18)	W–C(12)	199.4(9)
Pt–C(1)	194.6(7)	W–C(13)	203.7(9)
W–P(1)	250.8(2)	C(1)–N	123.7(9)
W–C(1)	231.2(7)		
<i>Bond angles</i>			
C(1)–W–C(13)	106.7(3)	P(2)–Pt–P(3)	106.14(7)
P(1)–C(26)–P(2)	110.5(4)	Pt–C(1)–W	83.2(3)
P(1)–W–C(11)	92.3(2)	Pt–W–C(1)	42.88(18)
P(1)–W–C(10)	169.6(2)	C(1)–W–C(10)	78.9(3)
P(1)–W–C(12)	88.6(3)	C(1)–W–C(11)	76.7(3)
P(1)–W–C(1)	109.58(19)	C(1)–W–C(12)	154.2(3)
P(1)–W–C(13)	86.5(2)	C(10)–W–C(11)	95.7(3)
W–Pt–P(3)	154.29(5)	C(10)–W–C(12)	85.6(4)
W–Pt–P(2)	99.34(5)	C(10)–W–C(13)	85.2(3)
P(1)–W–Pt	75.75(5)	C(11)–W–C(13)	176.6(3)
Pt–C(1)–N	139.1(6)	C(1)–N–C(2)	126.9(7)
W–C(1)–N	137.7(5)		

$[(OC)_3Fe]\{\mu-C=N-CH_2PO(OEt)_2\}(\mu-dppm)Pt(PPh_3)$ adopts now exclusively a bridging bonding mode, as indicated by a $\nu(C=N)$ vibration at 1648 cm^{-1} in the IR spectrum of **9**. Note that even for the Fe–Pt couple a terminal CNR bonding mode may be adopted upon

treatment with the strong σ -donating *t*-butyl isocyanide. [32] This yellow, stable compound was furthermore completely characterized by multinuclear NMR spectroscopy (Table 7) and an X-ray diffraction study.

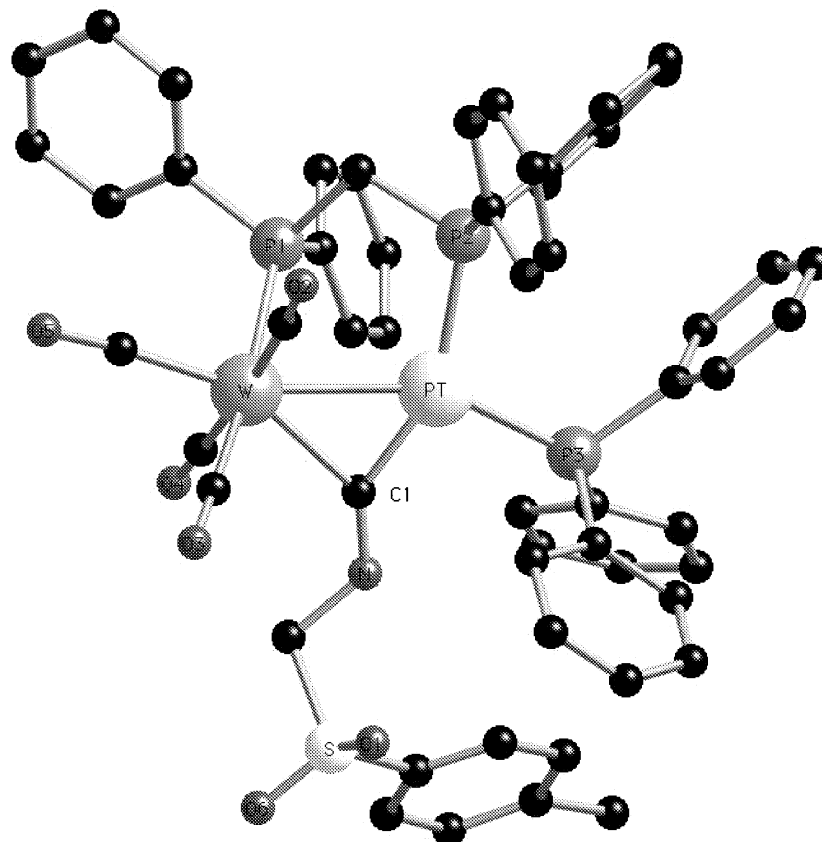
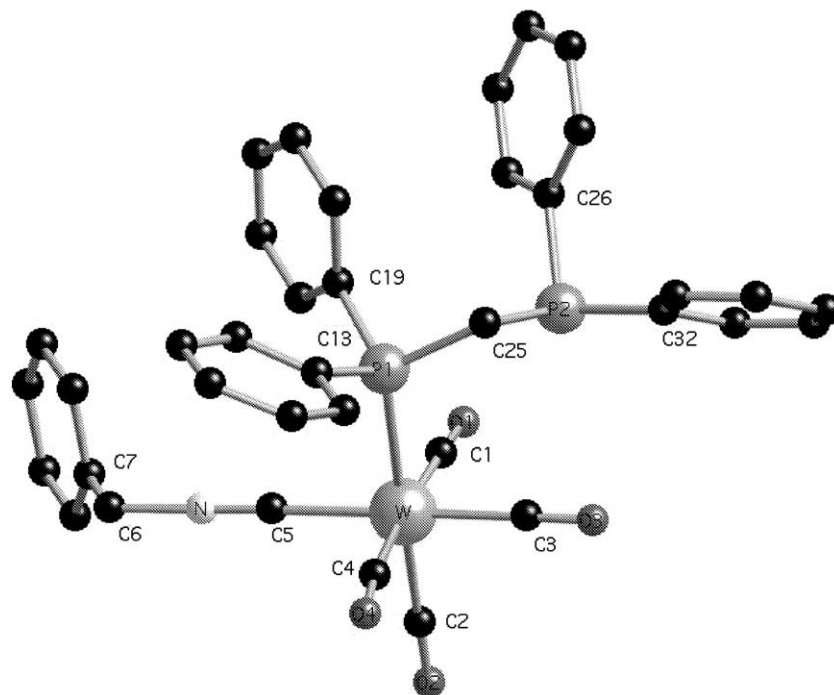


Fig. 4. View of the molecular structure of **3c** with the numbering scheme.

Fig. 5. View of the molecular structure of **8a** with the numbering scheme.Table 5
Selected bond lengths (pm) and bond angles (°) for **8a**

Bond lengths			
W–P(1)	252.4(2)	W–C(4)	206.9(8)
W–C(1)	207.8(8)	W–C(5)	213.3(8)
W–C(2)	200.9(8)	C(5)–N	111.7(10)
W–C(3)	203.2(8)		
Bond angles			
P(1)–W–C(1)	89.9(2)	P(1)–W–C(5)	87.0(2)
P(1)–W–C(2)	176.5(2)	C(5)–N–C(6)	179.0(2)
P(1)–W–C(3)	90.7(2)	P(1)–C(25)–P(2)	110.3(4)
P(1)–W–C(4)	92.0(2)		

3.4.1. Crystal structure of $[(OC)_3Fe\{\mu-C=N-CH_2PO(OEt)_2\}(\mu-dppm)Pt(PPh_3)]$ (**9**)

Suitable crystals of **9** were grown from CH_2Cl_2 -heptane. The molecular structure is depicted in Fig. 6, selected bond lengths and angles are given in Table 6. Since the overall geometry of **9** is quite reminiscent to that of the benzyl- and xylisocyanide bridged derivatives (obtained by other synthetic methods), only the most pertinent structural features will be discussed [11,14]. Like in the precursor $[(OC)_3Fe(\mu-C=O)(\mu-dppm)Pt(PPh_3)]$ [Fe–Pt 257.9(4) pm], the metal–metal bond of **9** [Fe–Pt 255.8(2) pm] is much shorter than that of **1a,c**, **2** and **3c**. As in the W–Pt system, the μ -CNR ligand is strongly bent [$121.4(5)^\circ$], the diethylphosphonate substituent being orientated towards the $Fe(CO)_3$ moiety. The bond length of the $C(1)=N$ double bond [$123.0(8)$ pm] is also very similar to that of **3c**. However,

the Pt– μ -C(1) distance of 200.1(6) pm is almost identical with the Fe– μ -C(1) distance of 200.6(6) pm resulting in a symmetric spanning of the two metals by the ligand. Due to the octahedral environment around Fe, the five-membered ring formed by P(1)–C(22)–P(2)–Pt–Fe is quite plane, the torsion angle P(1)–Fe–Pt P(2) being 6.83° .

Table 6
Selected bond lengths (pm) and bond angles (°) for **9**

Bond lengths			
Fe–Pt	255.8(2)	Fe–C(1)	200.6(6)
Pt–P(3)	226.5(3)	Fe–C(8)	178.0(8)
Pt–P(2)	232.1(2)	Fe–C(9)	175.3(7)
Pt–C(1)	200.1(6)	Fe–C(7)	179.2(8)
Fe–P(1)	224.2(2)	C(1)–N	123.0(8)
Bond angles			
C(1)–Fe–C(8)	83.9(3)	C(1)–N–C(2)	121.4(5)
P(1)–C(22)–P(2)	114.6(3)	Fe–Pt–P(3)	152.12(5)
P(1)–Fe–C(7)	86.8(2)	Fe–Pt–P(2)	97.67(7)
P(1)–Fe–C(8)	94.6(2)	P(1)–Fe–Pt	95.49(8)
P(1)–Fe–C(9)	106.8(2)	Pt–C(1)–N	138.2(5)
P(1)–Fe–C(1)	145.68(18)	C(1)–Fe–C(7)	88.0(3)
Fe–C(1)–N	142.4(5)	C(1)–Fe–C(9)	107.4(3)
P(2)–Pt–P(3)	110.08(8)	C(9)–Fe–C(8)	96.3(4)
Pt–C(1)–Fe	79.3(2)	C(9)–Fe–C(7)	95.0(4)
Pt–Fe–C(1)	50.25(17)	C(7)–Fe–C(8)	167.6(3)
Fe–Pt–C(1)	50.43(18)		

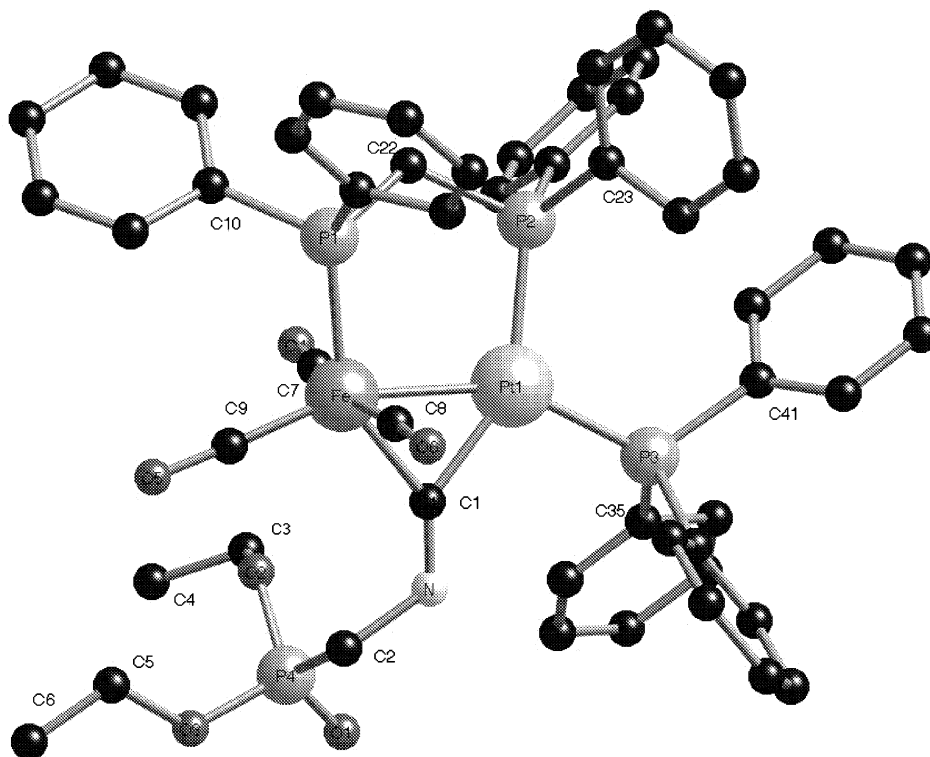


Fig. 6. View of the molecular structure of **9** with the numbering scheme.

3.5. Syntheses of μ -aminocarbonyl complexes

$[(OC)_4M\{\mu-CN(H)R\}(\mu-dppm)Pt(PPh_3)] [BF_4]$

Like their dppa-bridged homologues, **2** and **3b** are converted instantaneously and quantitatively to the cationic μ -aminocarbonyl complexes $[(OC)_4M(\mu-C=N(H)R')(\mu-dppm)Pt(PPh_3)][BF_4]$ (**10** and **11**) upon protonation with HBF_4 on the basic isocyanide nitrogen atom according to Scheme 4. [15,33]

This electrophilic addition of H^+ transforming μ -CNR into an excellently π -accepting aminocarbonyl ligand, enhances significantly the stability of the complexes, allowing now the recording of ^{13}C -NMR data. The resonance of the μ -carbonyl carbon of **11** was detected at δ 327.8 (dd, $^2J_{P,C} = 11, 67$ Hz) together with three sets of doublets for terminal carbonyl ligands at δ 207.8 (1 CO), 207.3 (1 CO, partially superimposed with the first carbonyl resonance) and 205.5 (2 CO, $^2J_{P,C} = 9$ Hz). A broad doublet at δ 75.2 ($^4J_{P,C} = 12$ Hz) is assigned to the NCH_2 carbon, and a singlet at δ 21.8 to the methyl carbon of the tosyl group. The following trends in the $^{31}P\{^1H\}$ -NMR and $^{195}Pt\{^1H\}$ -NMR spectra of **10** and **11** are apparent from Table 7: (i) in comparison with the precursors **2** and **3b**, the ddd resonance of the ^{195}Pt nucleus is shifted to ca. 300 ppm to lower field (**3b** δ -2594; **11** δ -2286); (ii) the resonances of P^1 and P^2 in the $^{31}P\{^1H\}$ -NMR are shifted to higher field; (iii) the $^{3+4}J_{P,P}$ couplings are reduced, whereas the $^{2+3}J_{Pt,P}$ couplings increase markedly.

4. Conclusion

This empirical study has shown that the bonding mode of the isocyanide ligand in complexes of the type $[(OC)_4M(CNR)(\mu-Ph_2PXPPH_2)Pt(PPh_3)]$ ($X = NH, CH_2$; $M = Cr, Mo, W$) depends exclusively on the electronic propensities of the organic substituents R of CNR ligand. Only in the case of very strongly withdrawing substituents R , an asymmetric bridging bonding mode is adopted. Even in the case of R groups, which are considered moderately electron donating, a terminal CNR bonding mode with conservation of the μ -CO bridge is preferred. This contrasts with the behaviour of $[(OC)_3Fe(\mu-CO)(\mu-Ph_2PXPPH_2)Pt(PPh_3)]$ towards CNR, where even CNR ligands with good donor propensities such as $R = xylyl$ or $benzyl$ adopt solely a symmetric μ -CNR bonding mode.

5. Supplementary material

Crystallographic data for the structural analysis have been deposited with the Cambridge Crystallographic Data Centre, CCDC nos. 206696 and 207729–207733 for compounds **2**, **1a**, **1c**, **3c**, **8** and **9**, respectively. Copies of this information may be obtained free of charge from The Director, CCDC, 12 Union Road, Cambridge CB2 1EZ, UK (Fax: +44-1223-336033; e-

Table 7

Selected $^{31}\text{P}\{^1\text{H}\}$ - and $^{195}\text{Pt}\{^1\text{H}\}$ -NMR data (δ in ppm and J in Hz; for all W–Pt compounds, the coupling constants given in this table correspond to J_{AB} , J_{AX} and J_{BX})

Complex	$\delta(\text{P}_\text{M})$	$\delta(\text{P}_\text{Pt})$	$\delta(\text{PPh}_3)$	$^2J_{\text{P,P}}$, $^2J_{\text{P,P}}$, $^3J_{\text{P,P}}$; $^1J_{\text{Pt,P}}$, $^1J_{\text{Pt,P}}$, $^2J_{\text{Pt,P}}$	$\delta(^{195}\text{Pt})$
1a (M = Cr)	55.9 dd	10.1 dd	45.1 dd	149, 61, 35; 3309, 4724 153, 63, 27; 3472, 4415, 65	–2431.5 dd
1b (M = Mo)	34.3 dd	15.1 dd	45.8 dd	160, 54, 17 4452, 3352, 41	–2514.5 ddd ^a
1c (M = W)	12.2 dd	14.0 dd	48.3 dd	129, 30, 31 4768, 2808, 15	–2484 ddd
2 (M = W) ^b	1.6 dd	2.9 dd	48.4 tq ^c	121, 42, 36; 4725, 2892 132, 41, 37; 4590, 3018	
3a (M = Cr)	46.9 dd	2.8 dd	42.8 dd	132, 36, 36 4573, 2966, 29	–2530 dd
3b (M = Mo)	26.0 dd	6.9 dd	43.6 dd	124, 33, 29 4526, 2849	
3c (M = W)	0.97 dd	5.33 dd	45.5 t	159, 50, 12 4456, 3340, 40	–2594 ddd
4 (M = W) ^d	0.8 dd	3.8 dd	44.2 dd	159, 54, 17 4486, 3342, 40	
5 (M = W)	11.7 dd	13.6 dd	48.0 dd	149, 31, 33 4230, 2876	–2490 ddd
6 (M = W)	12.6 dd	14.5 dd	48.8 dd	96; $^1J_{\text{W,P}} = 239$	–2507 ddd
7a (M = W) ^e	1.9 dd	6.3 dd	45.0 dd	90;	–2616 dd ^f
8a (M = W)	11.4 d, –25.2 d				
8b (M = W)	12.0 d, –24.4 d				
9 (M = Fe) ^g	70.7 dd	29.5 dd	39.6 dd	149, 26, 6; 4199, 2538, 60	–2598 ddd
10 (M = W)	–6.5 dd	–7.8 dd	39.49 dd	72, 25, 1; 4159, 2574, 73	
11 (M = Mo)	17.1 dd	3.4 dd	40.1 d	80, 22; 4346, 2549, 66	–2286 ddd

^a In $\text{C}_6\text{D}_6\text{--CH}_2\text{Cl}_2$.

^b ^{19}F -NMR: $\delta = -56$, s.

^c $^5J_{\text{F,P}} = 4$ Hz.

^d $\delta([\text{PPh}_3\text{CH}_2\text{NC}]^+) = 15.1$, s, $^4J_{\text{Pt,P}} = 22$ Hz.

^e $\delta(\text{PO}(\text{OEt})_2) = 21.2$, s.

^f $J_{\text{Pt,P}}^{2+3}$ not resolved.

^g $\delta(\text{PO}(\text{OEt})_2) = 23.6$, s.

mail: deposit@ccdc.cam.ac.uk or www: <http://www.ccdc.cam.ac.uk>

Acknowledgements

We are grateful to the Deutschen Forschungsgemeinschaft and the French Ministère de la Recherche et Technologie for financial support.

References

- [1] J.Y. Saillard, A.L. Beuze, G. Simmoneaux, P.L. Maux, G. Jaouen, *J. Mol. Struct.* 86 (1981) 149.
- [2] B.E. Bursten, R.F. Fenske, *Inorg. Chem.* 16 (1977) 963.
- [3] J.A. Howell, J.Y. Saillard, A.L. Beuze, G. Jaouen, *J. Chem. Soc. Dalton Trans.* (1982) 2533.
- [4] D. Lentz, *Angew. Chem. Int. Ed. Engl.* 33 (1994) 1315.
- [5] D. Lentz, M. Röttger, *J. Organomet. Chem.* 592 (1999) 41.
- [6] D. Lentz, S. Willemsen, *J. Organomet. Chem.* 612 (2000) 96.
- [7] J. Buschmann, D. Lentz, P. Luger, M. Röttger, G. Perpetuo, D. Scharn, S. Willemsen, *Z. Anorg. Allg. Chem.* 626 (2000) 2107.
- [8] M. Knorr, P. Braunstein, A. Tiripicchio, F. Ugozzoli, *J. Organomet. Chem.* 526 (1996) 105.
- [9] M. Knorr, C. Strohmann, *Eur. J. Inorg. Chem.* (1998) 495.
- [10] M. Knorr, C. Strohmann, P. Braunstein, *Organometallics* 15 (1996) 5653.
- [11] M. Knorr, C. Strohmann, *Eur. J. Inorg. Chem.* (2000) 241.
- [12] P. Braunstein, M. Knorr, G. Reinhard, U. Schubert, T. Stährfeldt, *Chem. Eur. J.* 6 (2000) 4265.
- [13] P. Braunstein, J. Durand, M. Knorr, C. Strohmann, *J. Chem. Soc. Chem. Commun.* (2001) 211.
- [14] M. Knorr, I. Jourdain, G. Crini, K. Frank, H. Sachdev, C. Strohmann, *Eur. J. Inorg. Chem.* (2002) 2419.
- [15] M. Knorr, C. Strohmann, *Organometallics* 18 (1999) 248.

Table 8
Crystallographic data

	1a	1c	2	3c	8a	9
Formula	C _{65.50} H _{55.50} CrO ₅ P ₃ Pt	C ₄₉ H ₃₉ Cl ₂ O ₅ P ₃ PtW	C ₄₉ H ₃₇ F ₃ NO ₄ P ₃ PtW	C _{57.50} H ₄₉ Cl ₃ NO ₆ P ₃ PtSW	C ₃₈ H ₃₀ Cl ₃ NO ₄ P ₂ W	C ₅₃ H ₅₁ Cl ₂ FeNO ₆ P ₄ Pt
<i>F</i> _w	1262.60	1250.55	1232.65	1460.24	916.77	1243.67
<i>T</i> (K)	173(2)	173(2)	153(2)	293(2)	173(2)	293(2)
Crystal size (mm ³)	0.20 × 0.20 × 0.10	0.20 × 0.20 × 0.10	0.14 × 0.09 × 0.04	0.20 × 0.10 × 0.10	0.20 × 0.20 × 0.10	0.20 × 0.20 × 0.10
Crystal system	Triclinic	Triclinic	Triclinic	Monoclinic	Monoclinic	Triclinic
Space group	<i>P</i> $\bar{1}$	<i>P</i> $\bar{1}$	<i>P</i> $\bar{1}$	<i>P</i> 2 ₁ / <i>n</i>	<i>P</i> 2 ₁ / <i>c</i>	<i>P</i> $\bar{1}$
Unit cell dimensions						
<i>a</i> (Å)	12.516(3)	11.146(7)	11.4307(14)	14.961(3)	9.0039(17)	11.779(8)
<i>b</i> (Å)	14.938(2)	11.879(9)	12.0368(15)	21.295(4)	39.092(15)	13.322(9)
<i>c</i> (Å)	17.160(4)	18.45(2)	19.095(2)	18.387(4)	10.708(2)	18.451(11)
α (°)	69.81(2)	79.33(12)	103.322(3)	90	90	86.88(5)
β (°)	71.97(3)	80.21(10)	97.823(3)	104.87(3)	99.81(2)	75.49(5)
γ (°)	79.02(3)	74.18(8)	110.848(3)	90	90	68.41(5)
<i>V</i> (Å ³)	2851.0(11)	2291(3)	2319.4(5)	5662(2)	3713.8(17)	2604(3)
<i>Z</i>	2	2	2	4	4	2
ρ calc (g.cm ⁻³)	1.471	1.813	1.765	1.713	1.640	1.586
μ (mm ⁻¹)	2.775	5.825	5.650	4.811	3.453	3.237
<i>F</i> (000)	1271	1208	1188	2852	1808	1244
θ Range (°)	2.15–27.00	2.26–26.00	1.89–27.00	1.57–22.50	2.19–25.00	1.65–23.99
Index ranges	–15 ≤ <i>h</i> ≤ 15, –19 ≤ <i>k</i> ≤ 19, –21 ≤ <i>l</i> ≤ 21	–12 ≤ <i>h</i> ≤ 13, –14 ≤ <i>k</i> ≤ 14, –22 ≤ <i>l</i> ≤ 22	–14 ≤ <i>h</i> ≤ 14, –15 ≤ <i>k</i> ≤ 15, –24 ≤ <i>l</i> ≤ 24	–16 ≤ <i>h</i> ≤ 15, 0 ≤ <i>k</i> ≤ 22, 0 ≤ <i>l</i> ≤ 19	–10 ≤ <i>h</i> ≤ 9, –46 ≤ <i>k</i> ≤ 46, –12 ≤ <i>l</i> ≤ 11	–12 ≤ <i>h</i> ≤ 13, –15 ≤ <i>k</i> ≤ 15, 0 ≤ <i>l</i> ≤ 21
Collected reflections	30617	15636	51804	7391	22326	8176
Independent reflections	11590	8433	10693	7391	6369	8176
Data/restraints/parameters	11590/0/687	8433/0/550	10693/0/559	7391/0/655	6369/0/424	8176/0/615
Largest difference peak and hole (e Å ⁻³)	1.155 and –1.729	2.653 and –5.337	1.846 and –0.990	1.195 and –0.664	1.085 and –1.651	1.414 and –1.665
Final <i>R</i> indices [<i>I</i> > 2 σ (<i>I</i>)]	<i>R</i> ₁ = 0.0326, <i>wR</i> ₂ = 0.0792	<i>R</i> ₁ = 0.0516, <i>wR</i> ₂ = 0.1300	<i>R</i> ₁ = 0.0255, <i>wR</i> ₂ = 0.0496	<i>R</i> ₁ = 0.0342, <i>wR</i> ₂ = 0.0748	<i>R</i> ₁ = 0.0455, <i>wR</i> ₂ = 0.1110	<i>R</i> ₁ = 0.0404, <i>wR</i> ₂ = 0.099
<i>R</i> indices (all data)	<i>R</i> ₁ = 0.0392, <i>wR</i> ₂ = 0.0814	<i>R</i> ₁ = 0.0606, <i>wR</i> ₂ = 0.1370	<i>R</i> ₁ = 0.0598, <i>wR</i> ₂ = 0.0585	<i>R</i> ₁ = 0.0482, <i>wR</i> ₂ = 0.0839	<i>R</i> ₁ = 0.0657, <i>wR</i> ₂ = 0.1182	<i>R</i> ₁ = 0.0499, <i>wR</i> ₂ = 0.1070
GOF on <i>F</i> ²	1.025	1.050	1.026	1.097	1.005	1.091

- [16] A.M. Bond, S.W. Carr, R. Colton, D.P. Kelly, *Inorg. Chem.* 22 (1983) 989.
- [17] T.S.A. Hor, *J. Organometal. Chem.* 319 (1987) 213.
- [18] J.W. Benson, R.L. Keiter, E.A. Keiter, A.L. Rheingold, G.P.A. Yap, V.V. Mainz, *Organometallics* 17 (1998) 4275.
- [19] U. Nagel, *Chem. Ber.* 115 (1982) 1998.
- [20] (a) G. Zinner, W.P. Fehlhammer, *Angew. Chem. Int. Ed. Engl.* 24 (1985) 979;
(b) D. Lentz, *J. Fluorine Chem.* 24 (1984) 523–530.
- [21] R.H. Blessing, *Acta Crystallogr. Sect. A* 51 (1995) 33.
- [22] (a) G.M. Sheldrick, *SHELXL-97*, Program for Crystal Structure Refinement. University of Göttingen, Germany.;
(b) G.M. Sheldrick, *SHELXS-97*, Program for Crystal Structure Solution. University of Göttingen, Germany.
- [23] G.B. Jacobsen, B.L. Shaw M. Thornton-Pett, *J. Chem. Soc. Dalton Trans.* (1987) 3079.
- [24] J.A.K. Howard, J.C. Jeffery, M. Laguna, R. Navarro F.G.A. Stone, *J. Chem. Soc. Dalton Trans.* (1981) 751.
- [25] (a) O. Bars, P. Braunstein, G.L. Geoffroy, B. Metz, *Organometallics* 5 (1986) 2021;
(b) P. Braunstein, C. de Méric de Bellefon, B. Oswald, M. Ries, M. Lanfrachi, A. Tiripicchio, *Inorg. Chem.* 32 (1993) 1638.
- [26] J. Powell, M.R. Gregg, J.F. Sawyer, *Inorg. Chem.* 28 (1989) 4451.
- [27] X.L.R. Fontaine, G.B. Jacobsen, B.L. Shaw M. Thornton-Pett, *J. Chem. Soc. Dalton Trans.* (1988) 741.
- [28] J.H. Davis, C.M. Lukehart, L. Sacksteder, *Organometallics* 6 (1987) 50.
- [29] T. Mizuta, M. Onishi, T. Nakazono, H. Nakazawa, K. Miyoshi, *Organometallics* 21 (2002) 717.
- [30] M.R. Awang, J.C. Jeffery F.G.A. Stone, *J. Chem. Soc. Dalton Trans.* (1983) 2091.